

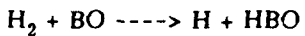
AD-A201 395

DTIC FILE COPY

(2)

OFFICE OF NAVAL RESEARCH
PROGRAM ELEMENT 61153N
TECHNICAL REPORT NO. 10

MULTIREFERENCE CONFIGURATION INTERACTION STUDY OF THE REACTION:



BY

Michael Page

Published

in the

Journal of Physical Chemistry

S DTIC
ELECTED OCT 25 1988 D
D C

Laboratory for Computational Physics
and Fluid Dynamics

NAVAL RESEARCH LABORATORY

WASHINGTON, DC 20375-5000

SEPTEMBER 1988

Reproduction in whole or in part is permitted for
any purpose of the United States Government

This document has been approved for public release
and sale, its distribution is unlimited

88 10 24 018

UNCLASSIFIED
SECURITY CLASSIFICATION OF THIS PAGE

REPORT DOCUMENTATION PAGE

1a. REPORT SECURITY CLASSIFICATION UNCLASSIFIED		1b. RESTRICTIVE MARKINGS NONE	
2a. SECURITY CLASSIFICATION AUTHORITY		3 DISTRIBUTION/AVAILABILITY OF REPORT UNLIMITED	
2b. DECLASSIFICATION/DOWNGRADING SCHEDULE			
4. PERFORMING ORGANIZATION REPORT NUMBER(S)		5 MONITORING ORGANIZATION REPORT NUMBER(S)	
6a. NAME OF PERFORMING ORGANIZATION Naval Research Laboratory	6b OFFICE SYMBOL (if applicable)	7a. NAME OF MONITORING ORGANIZATION Chemistry Division Office of the Chief of Naval Research	
6c. ADDRESS (City, State, and ZIP Code) Washington, DC 20375-5000		7b. ADDRESS (City, State, and ZIP Code) Arlington, VA 22217-5000	
8a. NAME OF FUNDING/SPONSORING ORGANIZATION ONR	8b. OFFICE SYMBOL (if applicable)	9. PROCUREMENT INSTRUMENT IDENTIFICATION NUMBER	
8c. ADDRESS (City, State, and ZIP Code)		10. SOURCE OF FUNDING NUMBERS	
		PROGRAM ELEMENT NO 61153N	PROJECT NO. RR013-01-4C
		TASK NO.	WORK UNIT ACCESSION NO.
11. TITLE (Include Security Classification) Multireference Configuration Interaction Study of the Reactions: $H_2 + BO \rightarrow H + HBO$			
12. PERSONAL AUTHOR(S) Michael Page			
13a. TYPE OF REPORT technical	13b. TIME COVERED FROM 9/87 TO 9/88	14. DATE OF REPORT (Year, Month, Day) September	15. PAGE COUNT
16. SUPPLEMENTARY NOTATION			
17. COSATI CODES		18. SUBJECT TERMS (Continue on reverse if necessary and identify by block number) → <i>B-BO, BOPIDE, CHEMICAL Reaction, JES</i>	
FIELD	GROUP	SUB-GROUP	
19. ABSTRACT (Continue on reverse if necessary and identify by block number) The reactants, transition state and products for the collinear abstraction reaction $H_2 + BO \rightarrow H + HBO$ have been studied using ab-initio MCSCF and multireference CI techniques with basis sets up to triple zeta plus double polarization quality. At the best level of theory, the reaction is calculated to be exothermic by 6.4 kcal/mole and have a zero point corrected barrier of 9.5 kcal/mole. Conventional transition state theory calculations of the rate coefficient with a tunneling correction through an Eckart barrier predict notable curvature in the Arrhenius plot over a wide temperature range. At low temperatures, this curvature is attributed to tunneling. At high temperatures, the curvature is attributed to the temperature dependence of the vibrational partition function caused by anomalously low doubly degenerate bending frequencies at the saddle point. The computed rate coefficient for the title reaction is well represented over a wide temperature range by the three parameter expression, $k(T) = 2.96 \times 10^{-22} T^{3.29} e^{-2200/T}$. A new and considerably more negative value of the standard heat of formation of HBO (-60 kcal/mole) is recommended.			
20. DISTRIBUTION/AVAILABILITY OF ABSTRACT <input checked="" type="checkbox"/> UNCLASSIFIED/UNLIMITED <input type="checkbox"/> SAME AS RPT. <input type="checkbox"/> DTIC USERS		21. ABSTRACT SECURITY CLASSIFICATION UNCLASSIFIED	
22a. NAME OF RESPONSIBLE INDIVIDUAL J. R. McDonald		22b. TELEPHONE (Include Area Code) (202) 767-3340	22c. OFFICE SYMBOL

Multireference Configuration Interaction Study of the Reaction:



Michael Page

Laboratory for Computational Physics
and Fluid Dynamics
Naval Research Laboratory
Washington, DC 20375

Abstract

The reactants, transition state and products for the collinear abstraction reaction $\text{H}_2 + \text{BO} \longrightarrow \text{H} + \text{HBO}$ have been studied using ab-initio MCSCF and multireference CI techniques with basis sets up to triple zeta plus double polarization quality. At the best level of theory, the reaction is calculated to be exothermic by 6.4 kcal/mole and have a zero point corrected barrier of 9.5 kcal/mole. Conventional transition state theory calculations of the rate coefficient with a tunneling correction through an Eckart barrier predict notable curvature in the Arrhenius plot over a wide temperature range. At low temperatures, this curvature is attributed to tunneling. At high temperatures, the curvature is attributed to the temperature dependence of the vibrational partition function caused by anomalously low doubly degenerate bending frequencies at the saddle point. The computed rate coefficient for the title reaction is well represented over a wide temperature range by the three parameter expression, $k(T) = 2.96 \times 10^{-22} T^{3.29} e^{-2200/T}$. A new and considerably more negative value of the standard heat of formation of HBO (-60 kcal/mole) is recommended.



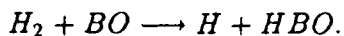
By _____
Distribution _____
Approved by _____
Date _____
A-1

I. Introduction

Solid boron and boron based materials are favorable candidates to be used as rocket fuels. This is because the efficient oxidation of boron to B_2O_3 releases considerably more chemical energy per unit volume of fuel than do conventional hydrocarbon based fuels. Among the practical bottlenecks to realizing this energy density advantage is that a substantial fraction of this chemical energy is trapped by gas phase formation of the HBO molecule. An understanding of the key factors controlling the branching between these two chemical pathways requires a detailed knowledge of the individual elementary reaction steps in the overall mechanism.

In sharp contrast to our knowledge of hydrocarbon chemistry, little is known about the homogeneous gas phase chemistry of boron/oxygen/hydrogen systems¹. Using the best available thermodynamic information, and estimating kinetic parameters, Brown and coworkers² have performed detailed kinetic modelling of boron oxidation. A set of individual reactions whose rates the modelling results were most sensitive to were singled out as deserving detailed study. Among these was the H atom abstraction from the HBO molecule by H_2O , and OH.

We report here a theoretical study of the reverse of one of the above reactions,



1

As discussed in a later section, our calculations predict the HBO molecule to be considerably more stable than previous estimates. A consequence of this is that in contrast to previous assertions, we predict reaction 1 to be exothermic. Following a description of electronic structure calculations in section II, sections III and IV report the computed structures, vibrational frequencies and energetics for reaction 1. The computed thermal rate coefficient for reaction 1 is found to deviate from Arrhenius temperature dependence at both low and high temperature. This temperature dependence of the reaction rate is presented and analyzed in section V. Finally the results are summarized and discussed in the last section.

II. Wavefunctions and Basis Sets

The electronic structure changes taking place during the course of reaction 1 are confined to a large extent to three electrons and three molecular orbitals (MO's). At the reactant, these are the hydrogen bonding and antibonding MO's and the associated pair of electrons and the sigma radical MO and electron at the boron site. At the product side, these are the BH bonding and antibonding MO's and hydrogen atom radical MO with their appropriate electron occupations. In a multiconfiguration self consistent field (MCSCF) description, these MO's and electron occupations smoothly change character during the course of the reaction, connecting these asymptotic descriptions in a continuous, qualitatively correct manner.

We choose as a reference description, a Complete Active Space Self Consistent Field (CASSCF)³ wavefunction involving 3 electrons and 3 active orbitals (3-in-3). This is an MCSCF wavefunction formed by including all possible doublet configurations distributing the three active electrons among the three active orbitals. There are 8 such configurations. The function of the reference description is threefold. First, it provides a qualitatively correct smoothly varying reference wavefunction as a base for large scale configuration interaction (CI) calculations. The CI is necessary to capture the detailed electron correlation effects required for accurate energetics. Second, the reference description is used to determine the location of the critical points on the potential energy surface, with the assumption that these do not change markedly at the CI level. Finally, the reference description is used to obtain potential energy surface information that is less critical than the overall energetics, such as vibrational frequencies for zero point vibrational energies and vibrational partition functions.

Overall energetics are determined from CI wavefunctions involving all single and double excitations from all eight reference configurations. The multireference (MR)CI wavefunctions employed in this study are all obtained within the frozen core approximation. That is, the molecular orbitals which correlate with the 1s core orbitals of boron and oxygen, along with the associated virtual orbitals are excluded in the configuration selection

and are thus forced to be doubly occupied and unoccupied respectively. MRCI wavefunctions such as those reported here have recently been shown, by detailed comparison to full CI wavefunctions in the same basis set, to provide accurate descriptions of bond breaking processes⁴.

Two basis sets are used in this study. The first, denoted DZP, is the standard Dunning 4s/2p contraction⁵ of the 9s/5p primitive set of Huzinaga⁶ on boron and oxygen with single d-polarization functions with exponents 0.70 on boron and 0.85 on oxygen and the corresponding unscaled 4s/2s contraction on hydrogen with a single p-function of exponent 0.75. The second basis set, denoted TZ2P is the 5s/3p contraction of the same gaussian primitive sets mentioned above augmented in each case with two sets of polarization functions with exponents of one half and double the DZP exponents. There are 42 contracted basis functions in the DZP basis set and 70 contracted functions in the TZ2P. The MRCI calculations described above include 106,000 configurations in the DZP basis set and 372,000 configurations in the TZ2P basis set.

The electronic structure calculations were all carried out on the Cray XMP-24 at the Naval Research Laboratory using the MESA⁷ system of programs

III. Structures and Vibrational Frequencies

Geometrical structures were fully optimized at the CASSCF/DZP level of theory for reactants, transition state and products of reaction 1. The results are tabulated in Table I. The saddle point is found to be linear and thus only bond lengths are reported. The BO bond length is found to remain nearly the same during the course of the reaction. This is consistent with the conjecture that except for the radical orbital and electron, the doubly bonded BO moiety remains fairly uninvolved in the reaction. Experimental bond lengths are shown in parentheses in Table I. None of the calculated bond lengths differ by more than .015 Å from the known experimental values. The predicted lengths both for the BH bond in HBO and the HH bond in molecular hydrogen are too long. In contrast, the predicted BO bond lengths for both boron monoxide and HBO are too short. These observations are reasonable when one considers that the reference 3-in-3 CASSCF wavefunction treats

the BO at essentially the Hartree Fock (HF) level throughout the reaction, and HF bond lengths are known to be short^{8,9}. At the reactant asymptote, the CASSCF wavefunction describes the BO by a spin restricted HF doublet wave function and molecular hydrogen by a 2-in-2 CASSCF. At the product, The HBO is asymptotically treated at the 2-in-2 CASSCF level, with the BH bond being correlated and the BO electrons essentially uncorrelated. The short BO bond lengths are thus consistent with expected HF results and the long BH and HH bonds are consistent with correlated bond lengths which are generally found to be too long with DZP quality basis sets^{8,9}.

At the saddle point on the potential energy surface, the HH bond is stretched by about 20% and the BH bond is stretched by about 28%. This is qualitatively consistent with Hammond's postulate. The transition state is marginally early but nearly centrally located, consistent with the calculated exothermicity of only about 8 kcal/mole at this level. This can be contrasted with the analogous H₂ + CN reaction for which the exothermicity is 25 kcal/mole and the HH and CH bonds are stretched by 10% and 50% respectively¹⁰.

Vibrational frequencies were determined by finite difference of the analytical CASSCF gradients with the DZP basis set. The results are shown in Table II along with the available experimental frequencies. As with the structural parameters, the deviations of the calculated frequencies from the experimental frequencies are consistent with known qualitative trends. Frequencies calculated at the HF level are generally found to be 10% or so too high, while introducing a modest amount of electron correlation at the MCSCF level yields frequencies that are too low. For the reactants the BO frequency, which is calculated at the HF level is about 10% too high and the H₂ frequency, which is calculated at the 2-in-2 CASSCF level is seen to be a few percent too low. For HBO, the stretching modes only approximately separate into a BH and a BO stretch. The BO stretching frequency is still essentially treated at the HF level and is found to be about 7% too high. The BH stretching frequency in HBO has not yet been assigned, but from these arguments one expects the calculated value of 2880 cm⁻¹ to be a little low.

The vibrational frequencies calculated at the transition state show some interesting

features, one of which has clear consequences for the temperature dependence of the rate coefficient. In a reaction path picture of chemical reactions, the vibrational frequencies and generalized normal modes change continuously along a path from reactant to product. Reactant, transition state and product frequencies and modes are thus adiabatically correlated with one another. The doubly degenerate bending mode in the product HBO (818 cm^{-1}) for example, arises out of zero frequency modes of the reactant. One might expect the frequency of this mode at the transition state to be between 0 and 818 cm^{-1} . For the analogous abstraction reactions, $\text{H}_2 + \text{OH}^{11}$ and $\text{H}_2 + \text{CN}^{10}$, this is the case but here it is not. This bending frequency is higher (980 cm^{-1}) at the saddle point than it is at the product. Likewise, one of the stretching frequencies drops considerably at the transition state below its value at the reactant or product. This behavior is also observed in $\text{H}_2 + \text{OH}^{11}$. The most interesting frequency value at the transition state is that of the low frequency degenerate bend (173 cm^{-1}). This mode correlates with zero frequency modes of both the reactant and product. Very low frequencies bends at the saddle point such as this have been found in other abstraction reactions which are very exothermic and consequently have very early transition states. For a series of similar reactions, a reasonable correlation was demonstrated between the frequency of these low frequency bends at the saddle point and the exothermicity of the reaction¹². It is reasonable to expect that if the saddle point is very early, the frequencies of these vibrational modes will tend to be low, since they arise out of zero frequency modes of the reactant. However, there is no a-priori reason to expect the converse of this conjecture to be true; that if the saddle point is not early, these modes will have higher frequencies. This is because they correlate with zero frequency modes of the products as well as the reactants. Indeed the present system does not fit this trend noted in reference 12. In a later section, we show how this unexpected low frequency manifests itself in the temperature dependence of the reaction rate coefficient.

Zero point vibrational energies, calculated from the unscaled harmonic frequencies are reported in Table II.

IV. Energetics

The enthalpy change accompanying reaction 1 is poorly resolved experimentally. Several determinations of the heat of formation for BO result in values ranging from -0.1 to 2.1 kcal/mole¹³. Following the recent thermochemical study of Brown² and the recommendation given in the JANAF thermochemical tables¹³, we adopt a value of 0.0 kcal/mole for this quantity. Assuming a standard heat of formation of 52.1 kcal/mole for the hydrogen atom, the enthalpy of reaction 1 becomes

$$\Delta H_{reaction\ 1}^{298} = 52.1 + \Delta H_f^{298}(HBO).$$

The heat of formation of HBO has previously been obtained only from thermochemical estimates. The value given in the JANAF tables¹³, -47 kcal/mole, predicts the reaction to be about 5 kcal/mole endothermic.

Our calculations, at all levels, predict reaction 1 to be exothermic, not endothermic. Calculated results for the activation energy and exoergicity of reaction 1 are presented in Table III at four different levels of theory. These include the 3-in-3 CASSCF (denoted MCSCF) with both the DZP and the TZ2P basis sets and MRCI with both basis sets. All entries in Table III are corrected for zero point vibrational energy differences. All energy calculations are done at the optimized MCSCF/DZP structures. The MCSCF wavefunction is designed to correctly describe the qualitative orbital changes during the reaction and is not expected to provide accurate energetics. Indeed, the MCSCF activation energy calculated with either basis set is seen to be quite high, 4.5 and 5.6 kcal/mole above the corresponding MRCI results for the DZP and TZ2P basis sets respectively. The overall reaction energy at the MCSCF level, on the other hand, is within 1 kcal/mole of the corresponding MRCI reaction energy for either basis set. These results are consistent with the often stated conjecture that electron correlation is more important in the transition region of a chemical reaction than at equilibrium configurations.

At the best level of theory, the computed zero point corrected barrier height and exothermicity for reaction 1 are 9.5 kcal/mole and 6.4 kcal/mole respectively. Using the calculated exothermicity and the assumptions discussed above, the standard heat of for-

mation for HBO can be obtained as -59 kcal/mole. We have recently completed a separate theoretical determination of this quantity¹⁴, based on the assumptions mentioned above and a fourth order Moller-Plesset perturbation theory calculation of the BH bond dissociation energy in HBO. This calculation leads to a heat of formation for HBO of -61 kcal/mole. These two procedures use distinct methods of reducing the liability of incomplete basis sets in bond dissociation energy calculations. In the calculations reported here, only an isodesmic energy comparison is made and in the perturbation theory calculations, a bond correction factor is included. We recommend a value for the standard heat of formation of $\Delta H_f^{298}(HBO) = -60$ kcal/mole, with the assumption that $\Delta H_f^{298}(BO) = 0.0$ kcal/mole.

Beyond some level of theory, basis set and electron correlation effects are expected to be relatively independent of one another and hence are expected to be additive. From Table III, the additivity assumption can be checked for the basis set enhancement DZP → TZ2P and the correlation enhancement MCSCF → MRCI. For the activation barrier, the value calculated by the additivity assumption (10.6 kcal/mole) is no more reliable than the MRCI/DZP barrier. The basis set effect predicted at the MCSCF level (2 kcal/mole) is twice as large as the basis set effect predicted at the MRCI level. For the reaction exergicity, for which the individual contributions are both smaller and in the same direction, the additivity assumption is seen to be better.

V. Temperature Dependence of the Rate Coefficient

The potential energy surface calculations described above provide enough information to calculate the thermal rate constant for reaction 1 using conventional transition state theory (TST)¹⁵ with a simple quantum correction for motion along the reaction coordinate. No attempt was made to account for variational effects in the location of the transition state¹⁶, for anharmonicity of the potential, or for more a rigorous investigation of the tunneling dynamics. All of these effects require descriptions of larger portions of the potential energy surface than are reported here. Although the combined influence of these effects on the rate constant can be fairly large¹⁶, they are still likely smaller than the error

induced by imprecise determination of the barrier height due to basis set and electron correlation deficiencies.

Within the approximation that reaction coordinate motion is separable from motion in the remaining degrees of freedom, the most reasonable barrier shape for describing tunneling dynamics is the vibrationally adiabatic ground state potential energy curve¹⁷. This is the sum of the potential energy of the reaction path and the zero point vibrational energies for the transverse vibrations at each point on the path. This again however, requires more potential energy surface information than is available here. Since these transverse vibrational frequencies can change substantially along the reaction path, the vibrationally adiabatic barrier can have a notably different shape from the bare barrier.

In this study, we fit an approximation to the adiabatic potential energy curve to the shape of an Eckart function^{15,17}. Since the zero point vibrational energies of the reactant, saddle point and product are known, the vibrationally adiabatic representation of the Eckart parameters, ΔV and V_b are known and are simply the zero point corrected exothermicity and the barrier height respectively. We do not know the one remaining parameter necessary to describe the Eckart function, the curvature of the vibrationally adiabatic barrier at the maximum. We approximate this quantity as follows, using the curvature of the bare barrier and the known zero point energies at the saddle point and at the asymptotes. The zero point energy, relative to its value at the saddle point is 0.6 kcal/mole at the reactant and 0.7 kcal/mole at the product. Assuming the potential energy about the saddle point is described by an inverted parabola with curvature equal to that of the bare barrier, the distance from the saddle point is found for which the potential energy drops to its value at the reactant. The zero point contribution to the vibrationally adiabatic potential is then assumed to fit a parabola which reaches the asymptotic zero point contribution (.65 kcal/mole) at this same distance from the saddle point. By this procedure, the approximate adiabatic barrier is predicted to be a little broader than the bare barrier, reducing the bare barrier force constant at the saddle point by about 7 %.

The curvature of the bare barrier is taken to be the curvature calculated at the MC-

SCF/DZP level, for which the force constants are available. Since the height of the adiabatic barrier at this level (13.0 kcal/mole) is greater than the best estimate of this quantity (9.5 kcal/mole), one expects the curvature to be a little bit too large. In addition, the influence of reaction path curvature on the tunneling probability is not considered in the calculations presented here. The effects of these two deficiencies are expected to increase and decrease the predicted tunnelling contribution respectively.

Given the parameters for the Eckart potential, the one dimensional quantum mechanical transmission probability is computed exactly at a large number of energies. The temperature dependent tunneling correction is then determined by converged numerical integration of the energy dependent transmission probabilities with a boltzmann factor.

The results of conventional TST calculations of the rate constant, using the harmonic oscillator approximation for the bound degrees of freedom and with the quantum correction described above are shown in Figure I. The solid line is an Arrhenius curve including the tunneling correction and the dotted line is the TST rate calculated without a correction for tunneling. At low temperatures, a substantial enhancement in the rate constant is predicted due to tunneling. This manifests itself as upward curvature in the Arrhenius plot of Figure I. The value of the rate constant in the temperature regime where tunneling is predicted to play an important role is quite small however. Tunneling is predicted to enhance the rate by a factor of 22 at 300°K and a factor of 1.3 at 1000°K. It is interesting to note that above about 2000°K, the quantum mechanical correction along the reaction coordinate *decreases* the computed rate constant. This is because non-classical reflection at energies above the barrier becomes more significant than tunneling at energies below the barrier.

Figure I also shows positive Arrhenius curvature at the higher temperatures of interest in combustion. This behavior is not due to tunneling but rather is due to the strong temperature dependence of the vibrational partition function. The anomalously low frequency bends at the saddle point become active at relatively low temperatures and essentially behave like classical oscillators. The activation energy (defined as $E_a = -Rd(\ln(k))/d(1/T)$)

is predicted to change by a almost factor of 4, from 6.4 to 24.2 kcal/mole, over the temperature range, 300K to 3000K. At low temperatures, this is due primarily to tunneling and at high temperatures it is due primarily to the temperature dependence of the vibrational partition function.

A breakdown of the various contributions to the activation energy is shown in Figure II. The total activation energy, which is the sum of all other curves, is represented as curve A. Curve B is the vibrationally adiabatic barrier height, i.e., the barrier height on the potential energy surface corrected for zero point vibrational energy differences. The contributions due to the low frequency degenerate bending modes and due to all the remaining modes of motion are shown as curves C and D respectively. Curve C essentially contributes the classical equipartition value of $2kT$ even at low temperatures. Curve E is the tunneling contribution to the activation energy. At low temperatures, the activation energy is seen to be lowered by over 3 kcal/mole due to tunneling. It is interesting to compare this to the computed effect of tunneling in the addition of a hydrogen atom to formaldehyde¹⁸. The potential energy barrier in that case was found to be 8.0 kcal/mole, similar to the 9.5 kcal/mole barrier for the present reaction. RRKM plus tunneling calculations were carried out for the reverse methoxy radical decomposition reaction. It was found that in order to reproduce these results using RRKM calculations without tunneling, the barrier had to be lowered by 3.5 kcal/mole.

The calculated rate constant is well represented ($\pm 10\%$) over the temperature range, 300K to 3000K by the three parameter fit,

$$k(T) = 2.96 \times 10^{-22} T^{3.29} e^{-2200/T}$$

VI. Summary and Conclusions

We present high level ab initio calculations of the reactant, saddle point and product for the reaction $H_2 + BO \rightarrow H + HBO$. Contrary to previous estimates, this reaction is predicted to be exothermic, with a 0°K exothermicity of 6.4 kcal/mole and barrier height

of 9.5 kcal/mole. The transition state is centrally located with the HH bond stretched by about 20% and the BH bond stretched by about 28%. The frequency of the doubly degenerate bending vibration at the transition state is found to be very low. As a consequence, this mode becomes *active* at relatively low energies. This is manifested as substantial upward curvature in the transition state theory Arrhenius plot at high temperatures. The Arrhenius plot is found also to be notably curved at low temperatures. This behavior is attributed to quantum mechanical tunneling. The computed rate is found to be well described over a wide temperature range by a three parameter fit. The rate calculations represent a prediction in the absense of experiment for this critical reaction in boron combustion.

Acknowledgment

This research was supported by Naval Research Laboratory and by the Mechanics Division of the Office of Naval Research

Table I
 MCSCF Structural Parameters
 for Hydrogen Atom Abstraction from HBO

	$R_{HH}(\text{\AA})$	$R_{BH}(\text{\AA})$	$R_{BO}(\text{\AA})$
$H + HBO$	∞	1.183 (1.168)	1.191 (1.200)
$H - - H - - BO$	0.905	1.519	1.191
$H_2 + BO$	0.756 (.742)	∞	1.193 (1.205)

experimental bond lengths (in parentheses) for HBO and BO are from references 20 and 21 respectively

Table II
MCSCF/DZP Vibrational Frequencies*

$H_2 + BO$	$H - - H - - BO$	$H + HBO$
2093 (1896)	1676 <i>i</i>	818 [2] (764)
4280 (4405)	173 [2]	1997 (1864)
	980 [2]	2880
	1461	
	2147	
ZPE**	9.1	8.5
		9.3

* cm^{-1} , experimental frequencies (in parentheses) are from reference 13 for H_2 and BO and reference 18 for HBO

** zero point vibrational energy (kcal/mole)

Table III
Activation Barrier and Exoergicity for $H_2 + BO \longrightarrow H + HBO^*$

	E_a^*	E_r^{**}
MCSCF/DZP	13.0	8.9
MCSCF/TZ2P	15.1	7.1
MRCI/DZP	8.5	7.9
MRCI/TZ2P	9.5	6.4

* zero point energy corrected activation barrier (kcal/mole)

** zero point energy corrected exoergicity (kcal/mole)

Figure Captions

Figure I. Temperature dependence of the computed rate coefficient for the reaction $H_2 + BO \rightarrow H + HBO$. The dashed curve is the result of conventional transition state theory calculations using *ab initio* potential energy surface information. The solid curve includes a quantum correction for motion along the reaction coordinate.

Figure II. Breakdown of the various contributions to the computed activation energy for the reaction $H_2 + BO \rightarrow H + HBO$ (see text).

REFERENCES

1. Faeth, G. M. "Status of Boron Combustion Research," Report of the Boron Combustion Specialists workshop, Air Force Office of Scientific Research, (October 1984)
2. Brown, R. C., Kolb, C. E., Yetter, R. A., Dryer, F. L., Rabitz, H. R. "Development of a Boron Assisted Combustion Model with Sensitivity Analysis, report prepared for Air Force Office of Scientific Research, March, 1987
3. P. E. M. Siegbahn, A. Heiberg, B. O. Roos, B. Levy, Phys. Scr., 21, 323 (1980); B. O. Roos, P. R. Taylor, P. E. M. Siegbahn, Chem. Phys., 48, 152 (1980)
4. see for example C. W. Bauschlicher, P. R. Taylor, J. Chem Phys., 86, 5600 (1987) and references therein
5. T.H. Dunning, Jr., J. Chem. Phys. 53, 2823 (1970); T.H. Dunning , P.J. Hay, in: Modern Theoretical Chemistry, Vol. 3. Methods of Electronic Structure Theory, ed. H.F. Schaefer III (Plenum Press, New York, 1977)
6. S. Huzinaga, J. Chem. Phys., 42, 1293 (1965)
7. MESA (Molecular Electronic Structure Applications), P. Saxe, B.H. Lengsfeld, R. Martin and M. Page
8. D. J. DeFrees, K. Raghavachari, H. B. Schlegel, J. A. Pople, J. Am. Chem. Soc., 104, 5576 (1982)
9. D. J. DeFrees, J. S. Binkley, A. D. Mclean, J. Chem. Phys., 80, 8 (1984)
10. R.A. Bair, T.H. Dunning, Jr., J. Chem. Phys. 82, 2280, (1985)
11. S. P. Walsh, T. H. Dunning, Jr., J. Chem. Phys., 72, 1303 (1980)
12. A. F. Wagner, R.A. Bair, Int. J. Chem. Kinet., 18, 473, (1986)
13. D.R. Stull, H. Prophet, Project Directors, JANAF Thermochemical Tables, 2nd ed. (US Government printing Office, Washington, DC, 1971), NSRDS-NBS 37, Catalog Number c13.48:37
14. M. Page, G. F. Adams, manuscript in preparation, This calculation employed a DZP

basis set and included a bond correction factor of 2.8 kcal/mole determined from calculated BH bond defects in boron hydrides

15. H. S. Johnston, "Gas Phase Reaction Rate Theory," Ronald Press, New York. 1966
16. D. Truhlar, A. Isaacson, B. Garrett, in "Theory of Reaction Dynamics," Vol. IV, M. Baer, ed., CRC Press, Boco Raton, Florida (1985), p. 65
17. C. Eckart, Phys. Rev., 35, 1303 (1930)
18. M. Page, M. C. Lin, Y. He, T. K. Choudhury, submitted to J. Phys. Chem., August, 1988
19. Y. Kawashima, K. Kawaguchi, E. Hirota, Chem. Phys. Lett., 131, 205, (1986)
20. Y. Kawashima, Y. Endo, K. Kawaguchi, E. Hirota, Chem. Phys. Lett., 135, 441, (1987)
21. M. Tanimoto, S. Saito, E. Hirota, J. Chem. Phys., 84, 1210, (1986)

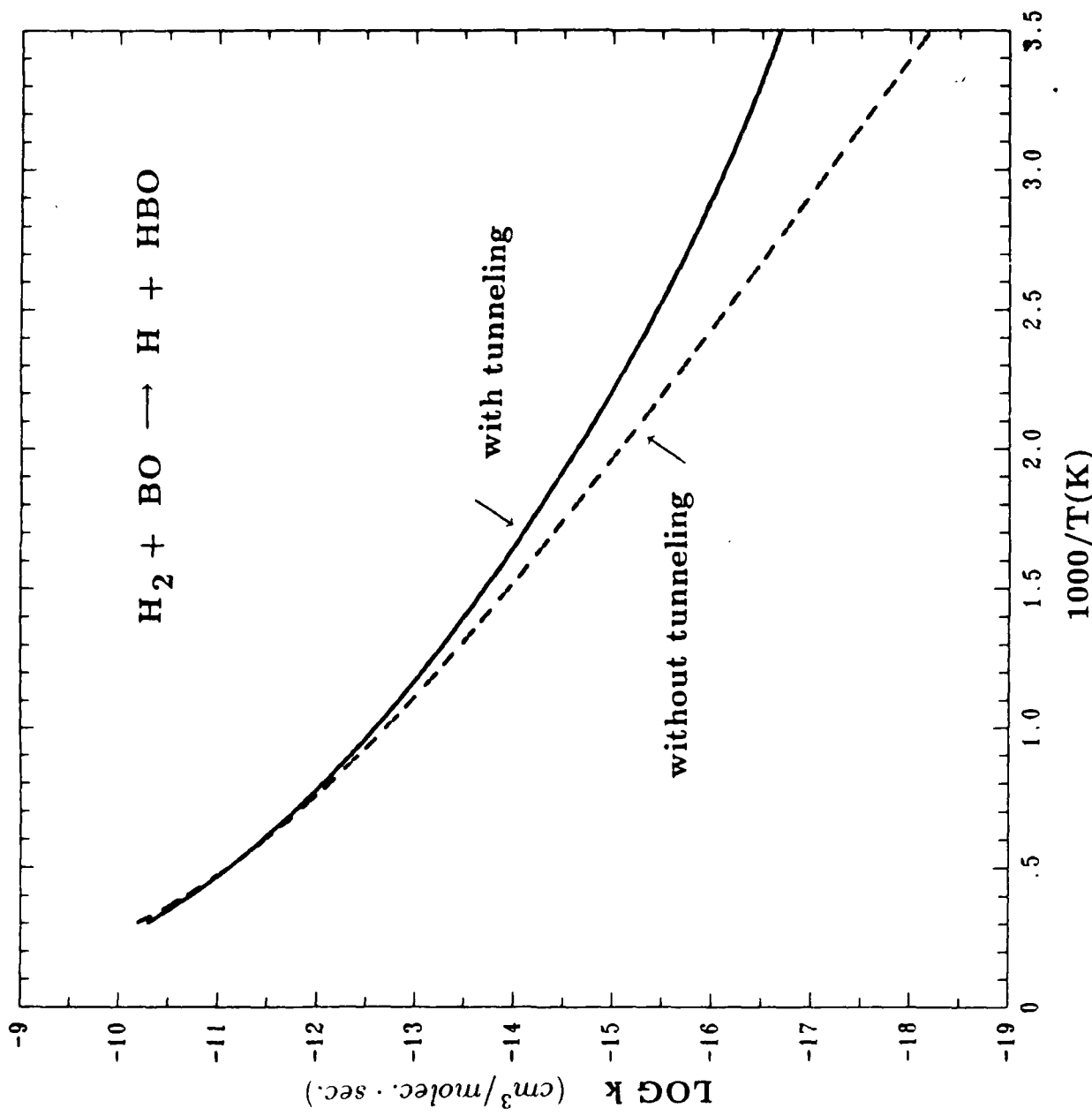


FIG-II

